PAPER

NJC
www.rsc.org/njc

Exchange coupling behavior of cyano-bridged binuclear Fe(III)–Ni(II) complexes: a density functional theory combined with broken-symmetry approach

Yi-Quan Zhang,*[a] Cheng-Lin Luo[a] and Zhi Yu[b]

[a] *School of Physical Science and Technology, Nanjing Normal University, Nanjing, 210097, China. E-mail: zhangyiquan@pine.njnu.edu.cn*

[b] *State Key Laboratory of Coordination Chemistry, Coordination Chemistry Institute, Nanjing University, Nanjing, 210093, China*

Received (in Montpellier, France) 21st June 2005, Accepted 9th August 2005
First published as an Advance Article on the web 30th August 2005

Molecular magnetism in a series of cyano-bridged Fe(III)–Ni(II) complexes has been investigated using hybrid density functional theory (DFT) B3LYP combined with broken symmetry (BS) approach. Two structural factors of the r distance (Ni–N_{brid}) and the θ angle (Ni–N_{brid}–C_{brid}) on J are analyzed by us in detail. The calculated results show that the J values increase with the increase of the r distance when the θ angles are smaller than 150°. When θ is 150°, the J values are almost the same for the different r distances. However, when θ is larger than 150°, the J values will decrease with the increase of the r distance. However, for all of the r distances, the J values will decrease with the increase of the θ angle except for when the θ angles are in the range 120–130° or 170–180°. Then we use above trends to interpret the experimental and calculated J values of the complete structures for a series of cyano-bridged Fe(III)–Ni(II) complexes. In addition, we find that Fe(III) mainly displays its polarization effect and although the largest part of the spin density is located at the Ni(II), there is an important delocalization of the unpaired electron, mostly to the six donor atoms, through the calculated spin density distributions.

Introduction

In molecular magnetism, the magneto-structural correlation of bridged transition metal dimers has received considerable attention both experimentally and theoretically.[1] One of the most extensively studied families experimentally, owing to their special structures, is that of the cyano-bridged transition metal complexes. A number of cyano-bridged transition metal complexes have been synthesized,[2] among which, cyano-bridged Fe(III)–Ni(II) complexes have been received much attention recently.[3–12] The variable temperature magnetic susceptibility data show that these complexes have weak intramolecular ferromagnetic exchange interactions with coupling constants J in the range 0–10 cm^{-1}. A wide range of Ni–N_{brid}–C_{brid} angles could stabilize ferromagnetic Fe(III)–Ni(II) coupling through the CN^- bridge. As usual, the Ni–N_{brid}–C_{brid} angles are larger as the Ni–N_{brid} distances are shorter from the experimental structures and the J values become larger with the increase of the Ni–N_{brid}–C_{brid} angles. So some experimental chemists consider that the smaller J values might be attributed to the more bent Ni–N_{brid}–C_{brid} linkages.[7] However, the effect of the Ni–N_{brid} distance is not considered by them. In our paper, we will investigate the dependence of J with the Ni–N_{brid} distance and Ni–N_{brid}–C_{brid} angle.

The existence of a manifold of states separated by small energy difference makes the evaluation of the energy of cyano-bridged Fe(III)–Ni(II) complexes difficult within a monodeterminant method. Sophisticated post-Hartree–Fock methods such as CASSCF,[13,14] CASPT2,[13,14] and DDCI[15] have been shown to provide good approximations to coupling constants, but the huge demand of computational resources associated with these methods severely limits their applicability to most of the complexes of actual experimental interest.[16–21] So methods based on density functional theory (DFT) have been shown to be simply more convenient.[22,23] In this paper, we use density functional theory (DFT) combined with the broken-symmetry (BS) approach proposed by Noodleman [24–26] to investigate the magneto-structural correlations for a series of cyano-bridged Fe(III)–Ni(II) complexes.

As a first step in the study of magneto-structural correlations of cyano-bridged Fe(III)–Ni(II) complexes, we have chosen the general topology represented in **1** which is found in complexes **A–G** (Table 1). First we report calculations of the exchange coupling constants for the complete structures and compare the results with the experimental data. Then we will analyze the effect of two structural factors on the exchange coupling in both the modeled structures of model **1** and the modeled compounds of complexes **B**, **C**, **D**, **G2**, **G3** and **H**: (1) the Ni–N_{brid} distance (2) the Ni–N_{brid}–C_{brid} angle. Molecular orbital analysis will be discussed for compound **D**. Finally, we will discuss the calculated spin density distributions of complex **D**.

Computational methodology

Description of the complexes and models

Considering the computational resources, we extracted those structures that only include one exchange pathway of Fe(III) and Ni(II) from one-, two- or three-dimensional cyano-bridged Fe(III)–Ni(II) complexes. To be able to compare our calculated coupling constants for complete structures with the experimental values, we used the molecular structures which are the crystallographic results rather than the optimized ones, because small changes to the experimental structures could result in significant deviations for the coupling constants. Fig. 2 depicts the structure of complex **D** (not including H atoms). The complex is made of one macrocyclic $[Ni(H_2L)]^{4+}$ (L = 3,10-bis(2-aminoethyl)-1,3,6,8,10,12-hexaazacyclotetra-

DOI: 10.1039/b508802j

Table 1 Experimental and calculated J values for all of the complete structure complexes

Cmpd		$Ni–N_{brid}$ / Å	$Ni–N_{brid}–C_{brid}$ / degree	J_{calc}/ cm^{-1}	J_{exp}/ cm^{-1}	Ref.
A		2.207	118.0	24.5	9.4	6
B		2.147	119.8	17.9		7
C		2.138	130.5	22.8		7
D		2.123	150.5	7.4	2.1	8
E		2.102	153.4	7.7	2.4	8
F		2.049	151.7	8.7	3.3	10
	G1	2.069	154.8	15.2		
G	**G2**	2.065	172.3	−8.1	5.3	11
	G3	2.017	165.6	7.2		
H		2.003	168.2	7.5		10
I		2.012	178.7	8.9	5.5	12

decane, 18-C-6 = 18-crown-6-ether) linked by one $[Fe(CN)_6]^{3-}$. The Ni–N1–C1 (C1N1 is the bridging ligand) angle is 150.48° and the Ni–N1 distance is 2.123 Å. The other complexes have similar structures to that of complex **D** only Ni linked by different terminal ligands. The nearest atoms to Ni are all N atoms except for the case of complex **I** and the $Fe–N_{brid}–C_{brid}$ angles are all about 170° for all of the complexes. To obtain the modeled structures of these complexes, we use NH_3 to substitute the nitrogen-coordinated ligands nearest to Ni. The structure of the general topology model **1** is similar to those of the other models. The $Ni–N_{term}$ distance has been taken as 2.074 Å, the average value found in the experimentally determined structures. For the ammonia molecules, the geometrical parameters that were used are $H–N_{term}$=1.028 Å. An average distance of 1.374 Å was taken for the bridge C–N bond length. The mean distance of the Fe–C bond is 1.944 Å and the $Fe–C_{term}$ bond is 1.930 Å. The mean distance of the terminal ligands C–N was 1.145 Å. An average angle of 173.17° was taken for the $Fe–C_{brid}–N_{brid}$ angle. The $Ni–N_{brid}$ distance and the $Ni–N_{brid}–C_{brid}$ angle will be changed for investigating magneto-structural correlations later. So we took 2.06 Å for the $Ni–N_{brid}$ distance and 180° for the $Ni–N_{brid}–C_{brid}$ angle at random. The $Ni–N_{brid}$ distance and the $Ni–N_{brid}–C_{brid}$ angle ranges from 2.00 Å to 2.20 Å and from 120° to 180°, respectively, according to the experimental data. In the next sections, we use θ and r to represent the $Ni–N_{brid}–C_{brid}$ angle and the $Ni–N_{brid}$ distance, respectively.

Calculation on exchange coupling constant

The magnetic interaction between Fe(III) and Ni(II) is studied on the basis of density functional theory coupling with the broken symmetry approach. The exchange coupling constants J have been evaluated by calculating the energy difference between the high-spin state (E_{HS}) and the broken symmetry state (E_{BS}).

Assuming the spin Hamiltonian is defined as:

$$\hat{H} = -2J\hat{S}_1 \cdot \hat{S}_2 \qquad (1)$$

according to recent Ruiz *et al.* experience based on a number of calculations on the magnetic exchange coupling constants with the broken-symmetry approach,[23,27,28] E_{BS} may be regarded as an approximation of the energy of the lowest spin state. They consider that local functionals overestimate the relative stabilization of the lowest spin state relative to the highest spin state,[29] DFT will usually give larger J values than experimental ones.[30,31] So Ruiz *et al.*[27] put forward the eqn (2) to calculate the J.

$$2J = \frac{E_{BS} - E_{HS}}{2S_1S_2 + S_2} \qquad (2)$$

however, this formula corresponds strictly to the limit of complete overlap between the magnetic orbitals and such a hypothesis is not sustained [32] although it can give the good J results compared to experiment.[23,27,28]

In a recent work,[33] Dai *et al.* examined the eigenstates of the Heisenberg spin Hamiltonian $\hat{H} = -2J\hat{S}_1 \cdot \hat{S}_2$ and the Ising spin Hamiltonian $\hat{H}^{Ising} = -2J\hat{S}_{1z}\hat{S}_{2z}$ for a general spin dimer consisting of M unpaired spins at one spin site and N unpaired spins at the other spin site. Their work shows that the description of the highest-spin and broken-symmetry spin states of a spin dimer by $\hat{H}$ is the same as that by $\hat{H}^{Ising}$. For the analysis of spin exchange interactions of a magnetic solid on the basis of density functional theory, the use of the Heisenberg spin Hamiltonian in the "cluster" approach is consistent with that of the Ising spin Hamiltonian in the "noncluster" approach. They put forward the eqn (3) according to the Heisenberg Spin Hamiltonian to calculate J. However, the same expression is also obtained by considering the energies of the HS and BS spin stated on the basis of the Ising spin Hamiltonian.

$$J = \frac{E_{BS} - E_{HS}}{MN} \qquad (3)$$

in our paper, we only select the cyano-bridged Fe(III)–Ni(II) complexes whose Fe(III) (d^5, t_{2g}^5) are all in the low-spin state. So $M = 2$ for Ni(II) and $N = 1$ for Fe(III), from the eqn (3) we further get the expression:

$$J = (E_{BS} - E_{HS})/2 \qquad (4)$$

We carry out calculations for molecules **A–I** and model **1** with Gaussian 98 computer code.[34] In the calculations of J using DFT-BS method, Illas *et al.*[35] showed the strong dependence of the calculated J with respect to the exchange-correlation functional chosen. In our paper, the popular hybrid B3LYP functional method proposed by Becke[36,37] and Lee *et al*[38] will be used to evaluate J. For the Fe(III) and Ni(II) ions, a basis set of triple-ξ quality[39] was used for the valence orbitals supplemented with two p orbitals ("polarization functions"), whereas a double-ξ basis set[40] was used for the other atoms in all of the complexes and models.

Results for full structures

The calculated coupling constants for the complete structures are presented in Table 1. Although compounds **B**, **C** and **H**

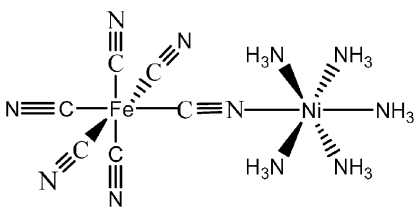

Fig. 1 Structure of model **1**.

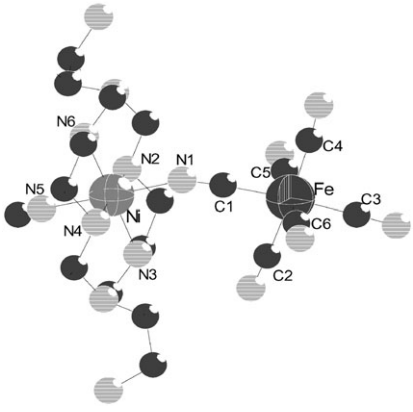

Fig. 2 Structure of complex **D**.

have no experimental J values, we also give the calculated ones. It can be seen that the calculated J values are qualitatively correct and empirically scale the J with respect to experiment. From the experimental and calculated data, we find the r distances often decrease and the J values often increase with the increase of the θ angle. And we also find the trend is correct only when the θ angles are larger than about 150°. In a recent work,[41] Kou *et al.* also found the same trend through experiment. In their work, all the θ angles of the compounds are also larger than 150°. However, for compounds **A**, **B** and **C** whose θ angles are all smaller than 150°, the above trend will not be suited. The exceptions of **A**, **B** and **C** will be investigated in the next section. For compounds **D–F**, their θ angles are almost the same, but the experimental J of compound **F** which has a shorter r distance is larger than those of **D** and **E**. From the calculated J of compounds **G1** and **G2** which have the similar r, the calculated J of compound **G1** is larger than that of **G2** although compound **G2** has a larger θ angle. From above analysis, we can find the r distance and the θ angle are both responsible for the J values. But how do the two structure factors of the r distance and θ angle have an influence on J? This will be investigated by us in detail in the next section.

Structural effects

To inspect the dependence of the magnetic behavior on the Ni–N_{brid}–C_{brid} angle, θ, we calculate the relevant J values with the θ angle ranging from 120° to 180° when the r distance is 2.00 Å, 2.06 Å, 2.12 Å, and 2.16 Å, respectively, for model **1**. The results are presented in Fig. 3(a) where the J values almost decrease with the increase of the θ angle for all of the r distances. Only when θ is equal to 120° or 180° have the J values departed a little from the trends. To further investigate the relationship between J and θ, we select the modeled structures of compounds **H** (r = 2.003 Å), **G2** (r = 2.065 Å), **D** (r = 2.123 Å) and **B** (r = 2.147 Å). The results are presented in Fig. 3(b) where the J values almost decrease with the increase of the angle for all of the modeled structures except for the θ angle being 120° or 180°.

Furthermore, we find the J values are almost negative when the Ni–N_{brid}–C_{brid} angles are from about 160° to 180° in Fig. 3. But the J values of the complete molecules are almost positive from Table 1. This is because the complete complexes in Table 1 have shorter r distances when these complexes have larger θ angles. In Fig. 3(a), when r is 2.00 Å (the shortest r distance in which we select) for model **1**, the J values are near positive when the θ angles are from about 160° to 180°. If we continue to decrease the r distance, the J values for model **1** will be positive for all of the θ angles. However, in Fig. 3, the selected r distances are all larger than 2.00 Å. So it is considerable the J values will be negative when θ angles are from about 160° to 180°. In Table 1, there is only one exception whose calculated J value is negative because it has a large θ angle (172.3°) and a long r distance (2.065 Å). Moreover, the limit case expected by us is not found when the Ni–N_{brid}–C_{brid} angles are 180° due to the orthogonality between the π system and "e_g" orbitals of Ni(II). This is because the Fe–C_{brid}–N_{brid} angles for model **1** (173.17°) and other modeled systems are not equal to 180°. They are not strictly orthogonalized between the π system and "e_g" orbitals of Ni(II) when the θ angles are 180°. So we don't find the expected limit case in Fig. 3 when the θ angles are 180°.

Above results tell us the J values almost decrease with the increase of the θ angle. But experimental data shows the J values often increase with the increase of the θ angle when θ is larger than 150°. This can be interpreted by investigating the relationship between J and r in the next part.

Fig. 4(a) represents the relationship between J and r when θ is 130°, 140°, 145°, 150°, 160°, 170° and 180°, respectively, for model **1**. The results show the J values are almost the same with the increase of the r distance when θ is about 150°. When θ is larger than 150°, the J values decrease with the increase of the r distance. However, the J values will increase with the increase of r when θ is smaller than 150°. To confirm the above results, we also give the relationship between J and r for the modeled structures of compounds **C** (θ = 130.53°), **D** (θ = 150.48°) and **G3** (θ = 165.64°). The results are presented in Fig. 4(b) where the J values have similar trends to those of model **1** with the increase of r .

Kahn's qualitative theory[42] can be used to interpret above results through the changes of the spin density on Ni(II). According to Kahn's theory, the exchange coupling constant J is expressed in eqn (5):

$$J_{ab} \approx K_{ab} + S_{ab}\,(\Delta^2 - \delta^2)^2 \qquad (5)$$

The positive term, K_{ab}, represents the ferromagnetic contribution J_F, favoring parallel alignment of the spins and a triplet ground state, while the negative term $S_{ab}\,(\Delta^2 - \delta^2)^2$ is the antiferromagnetic contribution J_{AF}, favoring antiparallel alignment of the spins and a singlet ground state. S_{ab} is the overlap integral between a and b. δ is the initial energy gap between the magnetic orbitals, Δ the energy gap between the molecular orbitals derived from them. When several electrons are present on each center, n_A on one side, n_B on the other, J can be described by the sum of the different 'orbital pathways' J_{ab}, defined as above for pairs of orbitals a and b located on each site, weighted by the number of electrons:

$$J = \textstyle\sum_{a,b} J_{ab}/n_A \times n_B \qquad (6)$$

As usual, the changes in the J_{AF} term are more important and these contributions usually will control the magneto-structural correlations. Hence, we only consider the changes in the J_{AF} term. From above eqn (5) and eqn (6), J_{AF} is associated to the overlap integral S_{ab} which is influenced by the

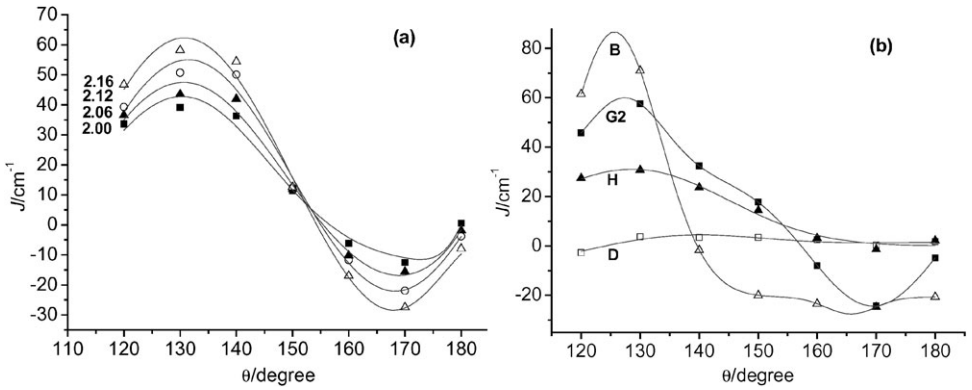

Fig. 3 **(a)** Magnetic coupling constant J as a function of the θ angle ranging from 120° to 180° for model **1** when r is 2.0 Å (■), 2.06 Å (▲), 2.12 Å (○) and 2.16 Å (Δ), respectively **(b)** Magnetic coupling constant J as a function of the θ angle ranging from 120° to 180° for the modeled structures of complexes **H** (r = 2.003 Å) (▲), **G2** (r = 2.065 Å) (■), and **D** (r = 2.123 Å) (□), **B** (r = 2.147 Å) (Δ), respectively.

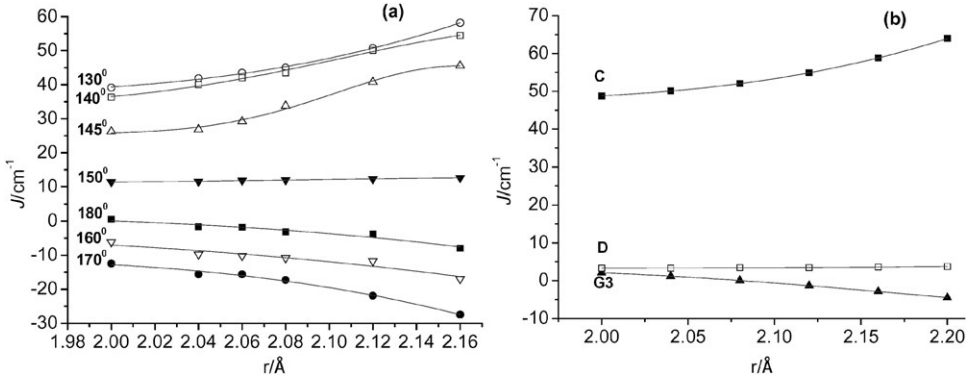

Fig. 4 **(a)** Magnetic coupling constant J as a function of the r distance ranging from 2.0 Å to 2.16 Å for model **1** when the θ angle is 130° (○), 140° (□), 145° (△), 150° (▼), 160° (▽), 170° (●) and 180° (■), respectively **(b)** Magnetic coupling constant J as a function of the r distance ranging from 2.0 Å to 2.20 Å for compounds **C** ($\theta = 130.53°$) (■), **D** ($\theta = 150.48°$) (□) and **G3** ($\theta = 165.64°$) (▲), respectively.

tropism of magnetic orbitals (the tuning or bending of the magnetic orbitals) and the delocalization of unpaired electrons. Because the spin populations on Fe(III) are always localized from our calculated results for all of the complexes and models, S_{ab} is associated to the spin delocalization of Ni(II).

We first investigated the relationship between J and the spin population ρ on Ni(II) in their high spin states for model **1** when the r distance is 2.00 Å, 2.06 Å, 2.12 Å and 2.16 Å, respectively, and for the modeled structures of compounds **H** ($r = 2.003$ Å), **G2** ($r = 2.065$ Å), and **D** ($r = 2.123$ Å) with the θ angles ranging from 120° to 180°. But we found the relationship between J and ρ is not clear for model **1** and also all of the modeled complexes. It is because the changes of θ will not only change the ρ on Ni(II) but also the tropism of magnetic orbitals. As we know, S_{ab} favoring antiferromagnetic contribution J_{AF} is not only associated to the spin delocalization of Ni(II) but also the tropism of magnetic orbitals. So it is understandable that the relationship between J and ρ is not clear.

Fig. 5 shows the relationship between J and ρ on Ni(II) in their highest spin states for model **1** when the θ angle is 130°, 140°, 145°, 150°, 160°, 170° and 180°, respectively, with the r distance ranging from 2.0 Å to 2.20 Å. In such cases, the changes of the distance r when the θ angle is fixed will not change the tropism of the magnetic orbital and only change ρ on Ni(II). So S_{ab} is only associated to ρ on Ni(II). For model **1** and the modeled structures, we find J increases with the increase of ρ when θ is smaller than about 150°. This can be easily rationalized using Kahn's qualitative theory. The increase of the ρ on Ni(II) will lead to the decrease of the absolute values of S_{ab} so as to the decrease of the J_{AF} term. And the J ($J = J_F + J_{AF}$) values which are positive will increase. However, the J values decrease with the increase of ρ when θ is larger than about 150° in Fig. 5. We consider that it is nearly orthogonal between the π system and "e_g" orbitals of Ni(II) in such large angles. So the J_{AF} term is small. As we know, K_{ab} is also associated to the overlap density which is influenced by ρ on Ni(II). When ρ increases, K_{ab} will decrease and, in turn, the J_F contribution will decrease. Therefore, the J ($J = J_F + J_{AF}$) values will decrease. But why are their J values almost negative in such conditions? It is due to the second-order perturbation corrections which favor antiferromagnetism. When θ is about 150°, K_{ab} and the absolute value of S_{ab} both decrease with the increase of ρ. Thus, the J values remain almost unchanged. We also investigated the relationship between J and ρ on Ni(II) in their highest spin states for the modeled structures of compounds **C** ($\theta = 130.53°$), **D** ($\theta = 150.48°$) and **G3** ($\theta = 165.64°$). They have similar trends to those of model **1**. However, we must point out the artifact of DFT will excessively delocalize the spin densities and B3LYP is not an exception,[43] although it gives the qualitatively correct result according to Kahn's theory with respect to experiment.

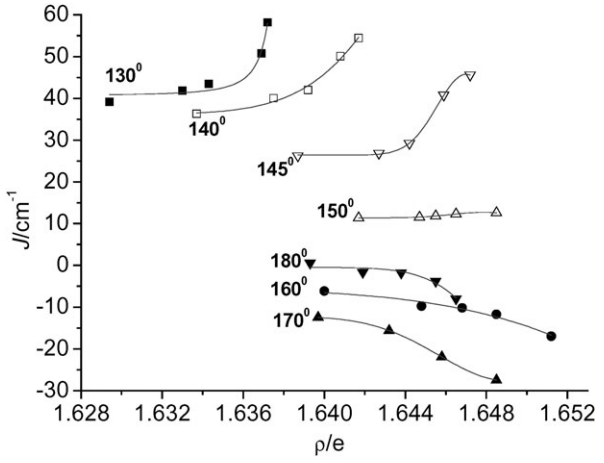

Fig. 5 Magnetic coupling constant J as a function of the spin population ρ on Ni(II) in its high spin state with the r distance ranging from 2.0 Å to 2.20 Å for model **1** when θ is 130° (○), 140° (□), 145° (△), 150° (▼), 160° (▽), 170° (●) and 180° (■), respectively.

From above analysis, we believe that the increase of the J values with the increase of the θ angle and the decrease of the r distance from the experimental data is due to a counteraction of the opposite effects which are the decrease of the r distance and the increase of the θ angle when the θ angles are larger than 150°. However, when the θ angles are smaller than 150°, the increase of the r distance will enhance the J values. So we find the calculated and experimental J values of compounds **A**, **B** and **C** from Table 1 are larger than those of others.

Now, we know why complexes **A**, **B** and **C** have larger J values than those of other complexes. They have smaller θ angles which are smaller than 150° and the longer r distances (when the angle is smaller than 150°, a longer r distance will give a larger J value). In the above sections, we discussed that when the θ angles are equal to 120° or 180°, the J values have a little departure from the trends. This can be confirmed by the calculated J values of complexes **B**, **C**, **G3**, **H** and **I**. For complexes **B** and **C**, they have the similar r distance, but the angle of complex **B** ($\theta = 119.8°$) is lower than that of complex **C** ($\theta = 130.5°$). So we understand why the J value of compound **B** is smaller than that of **C** (Table 1) from the trends in Fig. 3. The angle ($\theta = 178.7°$) of complex **I** is near to 180° and the angles of complexes **G3** and **H** are 165.6° and 168.2°, respectively, and they have the similar r distances. Also we know why the calculated J value of complex **I** is larger than those of complexes **G3** and **H** from the trends in Fig. 3.

Also, we can easily interpret why the calculated J value of **G2** is smaller than that of **G1** and the experimental J value of **F** is a little larger than those of **D** and **E** using the magneto-structure correlations between J and the two structural factors of the r

and θ investigated by us. Compound **G2** has a larger θ angle than that of **G1** and the r distances of **G1** and **G2** are almost the same. From the trends in Fig. 3, a larger θ angle will make for a smaller J value in the same r distance. So the J value of compound **G1** is larger than that of compound **G2**. For compounds **F**, **D** and **E**, their θ angles which are larger than 150° are almost the same. But compound **F** has a shorter r distance. From Fig. 5, a shorter r distance will make for a larger J value. So the J value of compound **F** is a little larger than those of compounds **D** and **E**.

Illas *et al.*[44] showed that the influence of terminal ligands on J is strongly dependent on exchange–correlation functionals, especially the hybrid B3LYP. They showed that B3LYP gave a large deviation of J when using NH_3 to substitute for the real ligands. However, we use B3LYP because the overall description and magnetostructural study is qualitatively correct and empirically scale the calculated J values with respect to experiment.

Molecular orbital analysis

In the above complexes that we studied, Fe^{III} (d^5) ions are all in the low-spin configuration. The unpaired electron in the Fe(III) is located in a t_{2g} orbital with only π-bonding character while in the case of Ni(II) cations, there is only one configuration, $(t_{2g})^6(e_g)^2$, with two unpaired electrons which are placed in antibonding orbitals. If the whole symmetry is high enough to retain the orthogonality of the t_{2g} and e_g orbitals ($< t_{2g} \mid e_g > = 0$), the Fe–Ni interaction will be ferromagnetic. For all of the complete structures that we studied except for complex **G2**, both the experimental and calculated results show the Fe–Ni interaction is ferromagnetic. The good agreement claimed in refs. 22 and 23 for the J values is based on the assumption of complete overlap of magnetic orbitals. However, for our studied systems in which the magnetic orbitals on Fe(III) and Ni(II) are strongly orthogonal, the assumption is not sustained.[32]

In Fig. 6, we show three α singly occupied molecular orbitals of complex **D** in its high spin state. The t_{2g} orbital (d_{xy}) where the unpaired electrons on Fe(III) are on the left and the two e_g orbitals ($d_{x^2-y^2}$ and d_{z^2}) where two unpaired electrons on Ni(II) are on the right. From Fig. 6, we find the d_{xy} orbital of Fe(III) displays zones of small magnitude around the bridges. According to the overlap density $\rho_{a_1b_1} = a_1(1)b_1(1)$ which favors ferromagnetic contribution, complex **D** should have a weak intramolecular ferromagnetic exchange interaction. This conclusion is consistent with the calculated and experimental J values of complex **D**. The other complexes also have such magnetic orbitals, so these complexes have weak intramolecular ferromagnetic exchange interactions with the coupling constants J in the range 0–10 cm^{-1}.

These singly occupied molecular orbitals are those that host the unpaired electrons, not necessarily those with the highest energy. This interpretation is supported by the analysis of the corresponding β orbitals for the α singly occupied molecular orbitals, which show no contribution at the Fe(III) and Ni(II) atoms. According to Kahn's theory,[45] only when the doubly occupied molecular orbitals are low in energy with respect to those singly occupied orbitals, the so-called kinetic exchange term which favoring antiferromagnetic generally dominates among the second-order perturbation corrections. From these orbitals, we find the singly occupied molecular orbital ϕ_1 where the unpaired electron on Fe(III) locates almost localized around Fe(III). For the singly occupied molecular orbitals ϕ_2 and ϕ_3 where two unpaired electrons on Ni(II) locate, there are non-negligible contributions at the bridges and Fe(III). This is due to the breakdown of the active electron approximation due to mixing of the orbitals in Fig. 6 with other occupied orbitals. The other complexes have similar singly occupied orbitals to those of complex **D**.

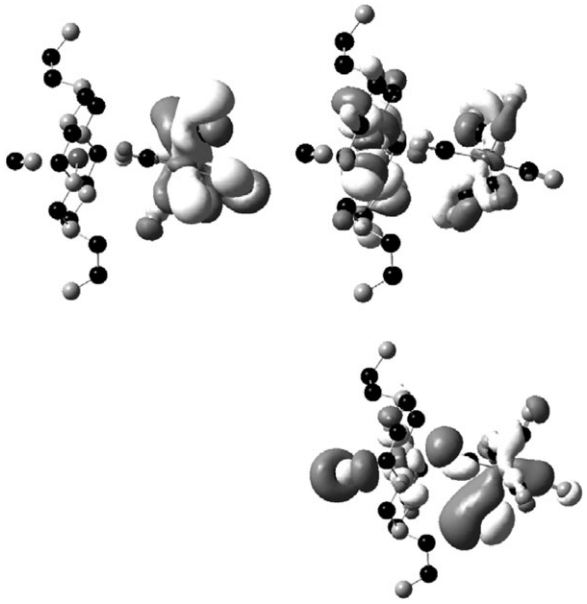

Fig. 6 Molecular orbitals bearing the unpaired electrons in the ferromagnetic state for complex **D**: one t_{2g} orbital on Fe(III) on the left, two e_g orbitals on Ni(II) on the right.

Spin density distribution

The spin density distributions obtained with Mulliken Population Analysis for the high-spin (HS) and broken-symmetry (BS) states of complex **D** are shown in Fig. 7 and the spin populations are shown in Table 2. The plus and minus signs indicate α and β spin states, respectively. It should be mentioned that the broken-symmetry state is a mixed spin state with $Ms = 0$, not to be a pure spin state, but it represents an averaged antiferromagnetic alignment of spins. The spin population on Fe(III) is 1.112 in HS state and −1.102 in BS state, which suggests the only one unpaired electron on Fe(III) is almost localized. The spin population on Ni(II) is 1.626 (HS) and 1.627 (BS) demonstrating a part of spin densities delocalization effect. In HS state, the spin population is −0.026 on the bridging atom C1 for the polarization of Fe and 0.053 on the bridging atom N1 for the delocalization of Ni(II). The spin populations of the terminal atoms C2, C3, C4, C5 and C6 nearest to Fe(III) are all negative. Thus Fe(III) mainly display its polarization effect. Although the largest part of the spin density is located at the Ni(II), there is an important delocalization of the unpaired electron, mostly to the six donor atoms. So, the spin populations of the terminal atoms N2, N3, N4, N5 and N6 around Ni(II) are all positive demonstrating the predominant delocalization effect from Ni(II). In BS state, the spin populations of the bridging and the terminal atoms nearest to Fe(III) and Ni(II) also show the predominant spin polarization from Fe(III) and delocalization from Ni(II). The spin density distributions of the other cyano-bridged Fe(III)–Ni(II) complexes are similar to those of complex **D**.

Fig. 7 Spin density maps calculated for complex **D** for the high spin (HS) state on the left and the broken-symmetry (BS) state on the right.

Table 2 Spin densities calculated for the high spin (HS) and broken-symmetry (BS) states of complex **D**

Atom	HS	BS	Atom	HS	BS
Fe	1.112	−1.102	N6	0.063	0.064
Ni	1.626	1.627	C1	−0.026	0.030
N1	0.053	0.057	C2	−0.038	0.038
N2	0.070	0.070	C3	−0.046	0.049
N3	0.077	0.077	C4	−0.057	0.058
N4	0.067	0.067	C5	−0.049	0.048
N5	0.040	0.040	C6	−0.056	0.055

Conclusions

Broken-symmetry approach combined with density functional theory succeeded in being applied to investigate the cyano-bridged Fe(III)–Ni(II) complexes. Most of these complexes have weak ferromagnetic interactions between Fe(III) and Ni(II) for the orthogonality of the magnetic orbitals of the low-spin Fe(III) (d^5, t_{2g}^5) and Ni(II) (d^8, $t_{2g}^6e_g^2$). Although the properly computed B3LYP value is too large and that comparison to experiment requires empirical scaling, the overall magnetos-tructural description appears to be qualitatively correct. As usual, the θ angle is larger as the r distance is shorter from the experimental structures. From our calculated results, we find the J values will decrease with the increase of the r distance when the θ angles are larger than 150°. However, when the θ angles are smaller than 150°, the J values will increase with the increase of the r distance. But for all of the r distances, the J values will decrease with the increase of the θ angle except for when the θ angles are in the range 120–130° or 170–180° (Fig. 3). This is why compounds **A**, **B** and **C** have such larger J values. From the above analysis, we know the smaller J values are not due to the more bent Ni–N_{brid}–C_{brid} linkages but the shorter Ni–N_{brid} distance. From the calculated spin density distributions, we find Fe(III) mainly displays its polarization effect and Ni(II) shows an important delocalization of the unpaired electron, mostly to the six donor atoms.

Acknowledgements

This project is supported by the National Natural Science Foundation of China (Grants G20001004, 19835050) and Natural Science Foundation of University of Jiangsu Province of China (Grant No. 05KJB150055). Thank Hui-Zhong Kou for helpful discussions.

References

1 (*a*) C. Desplanches, E. Ruiz, A. Rodriguez-Fortea and S. Alvarez, *J. Am. Chem. Soc*., 2002, **124**, 5197; (*b*) Z. D. Chen, Z. T. Xu, L. Zhang, F. Yan and Z. Y. Lin, *J. Phys. Chem. A*, 2001, **105**, 9710; (*c*) Q. H. Ren, Z. D. Chen, J. Ren, H. Y. Wei, W. T. Feng and L. Zhang, *J. Phys. Chem. A*, 2002, **106**, 6161; (*d*) Y. Q. Zhang, C. L. Luo and Z. Yu, *Int. J. Quantum Chem*., 2005, **102**, 165.
2 (*a*) M. P. Shores, J. J. Sokol and J. R. Long, *J. Am. Chem. Soc*., 2002, **124**, 2279; (*b*) J. J. Sokol, M. P. Shores and J. R. Long, *Inorg. Chem*., 2002, **41**, 3052; (*c*) L. G. Beauvais and J. R. Long, *J. Am. Chem. Soc*., 2002, **124**, 2110.
3 F. Bellouard, M. Clemente-León, E. Coronado, J. R. Gálan-Mascarós, C. J. Gómez-García, F. Romero and K. R. Dunbar, *Eur. J. Inorg. Chem*., 2002, 1603.
4 K. E. Vostrikova, D. Luneau, W. Wemsdorfer, P. Rey and M. Verdaguer, *J. Am. Chem. Soc*., 2000, **122**, 718.
5 J. Koo, D. Kim, Y. Kim and Y. Do, *Inorg. Chem*., 2003, **42**, 2983.
6 S. Juszczyk, C. Johansson, M. Hanson, A. Ratuszna and G. Malecki, *J. Phys.: Condens. Matter*, 1994, **6**, 5697.
7 E. Coronado, C. J. Gómez-Garcta, A. Nuez, F. M. Romero, E. Rusanov and H. Stoeckli-Evans, *Inorg. Chem*., 2002, **41**, 4615.
8 H. Z. Kou, B. C. Zhou, D. Z. Liao, R. J. Wang and Y. D. Li, *Inorg. Chem*., 2002, **41**, 6887.
9 E. Colacio, J. M. Domínguez-Vera, F. Lloret, A. Rodríguez and H. Stoeckli-Evans, *Inorg. Chem*., 2003, **42**, 6962.
10 C. P. Berlinguette, J. R. Galán-Mascarós and K. R. Dunbar, *Inorg. Chem*., 2003, **42**, 3416.
11 K. V. Langenberg, S. R. Batten, K. J. Berry, D. C. R. Hockless, B. Moubaraki and K. S. Murray, *Inorg. Chem*., 1997, **36**, 5006.
12 J. J. Yang, M. P. Shores, J. J. Sokol and J. R. Long, *Inorg. Chem*., 2003, **42**, 1403.
13 H. Y. Wei, B. W. Wang and Z. D. Chen, *Chem. Phys. Lett*., 2005, **407**, 147.
14 C. de Graaf, C. Sousa, I. de P. R. Moreira and F. Illas, *J. Phys. Chem. A*, 2001, **105**, 11371.
15 (*a*) J. Miralles, J. P. Daudey and R. Caballol, *Chem. Phys. Lett*., 1992, **198**, 555; (*b*) J. Miralles, O. Castell, R. Caballol and J. P. Malrieu, *Chem. Phys*., 1993, **172**, 33.
16 H. B. Schlegel and M. A. Robb, *Chem. Phys. Lett*., 1982, **93**, 43.
17 (*a*) K. Andersson, P.-A. Malmqvist and B. O. Roos, *J. Chem. Phys*., 1992, **96**, 1218; (*b*) K. Andersson, P.-A. Malmqvist and B. O. Roos, *J. Phys. Chem*., 1990, **94**, 5483.
18 O. Castell, R. Caballol, V. M. Garcia and K. Handrick, *Inorg. Chem*., 1996, **35**, 1609.
19 O. Castell and R. Caballol, *Inorg. Chem*., 1999, **38**, 668.
20 A. Ceulemans, L. F. Chibotaru, G. A. Heylen, K. Pierloot and L. G. Vanquickenborne, *Chem. Rev*., 2000, **100**, 787.
21 K. Fink, C. Wang and V. Staemmler, *Inorg. Chem*., 1999, **38**, 668.
22 E. Ruiz, P. Alemany, S. Alvarez and J. Cano, *J. Am. Chem. Soc*., 1997, **119**, 1297.
23 E. Ruiz, P. Alemany, S. Alvarez and J. Cano, *Inorg. Chem*., 1997, **36**, 3683.
24 L. Noodleman, *J. Chem. Phys*., 1981, **74**, 5737.
25 L. Noodleman and E. J. Baerends, *J. Am. Chem. Soc*., 1984, **106**, 2316.
26 L. Noodleman and D. A. Case, *Adv. Inorg. Chem*., 1992, **38**, 423.
27 E. Ruiz, J. Cano, S. Awarez and P. Alemany, *J. Comput. Chem*., 1999, **20**, 1391.
28 A. Rodriguez-Fortea, P. Alemany, S. Alvarez and E. Ruiz, *Chem. Eur. J*., 2001, **7**, 627.
29 G. L. Gutsev and T. Ziegler, *J. Phys. Chem*., 1991, **95**, 7220.
30 L. Noodleman, D. A. Case and A. Aizman, *J. Am. Chem. Soc*., 1988, **110**, 1001.
31 J. M. Mouesca, J. L. Chen, L. Noodleman, D. Bashford and D. A. Case, *J. Am. Chem. Soc*., 1994, **116**, 11898.
32 R. Caballol, O. Castell, F. Illas, I. de P. R. Moreira and J. P. Malrieu, *J. Phys. Chem. A*, 1997, **101**, 7860.
33 D. D. Dai and M. –H. Whangbo, *J. Chem. Phys*., 2003, **118**, 29.
34 M. J. Frisch, G. W. Trucks, H. B. Schlegel, G. E. Scuseria, M. A. Robb, J. R. Cheeseman, V. G. Zakrzewski, J. A. Montgomery, Jr., R. E. Stratmann, J. C. Burant, S. Dapprich, J. M. Millam, A. D. Daniels, K. N. Kudin, M. C. Strain, O. Farkas, J. Tomasi, V. Barone, M. Cossi, R. Cammi, B. Mennucci, C. Pomelli, C. Adamo, S. Clifford, J. Ochterski, G. A. Petersson, P. Y. Ayala, Q. Cui, K. Morokuma, D. K. Malick, A. D. Rabuck, K. Raghavachari, J. B. Foresman, J. Cioslowski, J. V. Ortiz, A. G. Baboul, B. B. Stefanov, G. Liu, A. Liashenko, P. Piskorz, I. Komaromi, R. Gomperts, R. L. Martin, D. J. Fox, T. Keith, M. A. Al-Laham, C. Y. Peng, A. Nanayakkara, C. Gonzalez, M. Challacombe, P. M. W. Gill, B. G. Johnson, W. Chen, M. W. Wong, J. L. Andres, M. Head-Gordon, E. S. Replogle and J. A. Pople, *GAUSSIAN 98 (Revision A.9)*, Gaussian, Inc., Pittsburgh,PA, 1998.
35 R. L. Martin and F. Illas, *Phys. Rev. Lett*., 1997, **79**, 1539.
36 A. D. Becke, *J. Chem. Phys*., 1993, **98**, 5648.
37 A. D. Becke, *Phys. Rev. A*, 1988, **38**, 3098.
38 C. Lee, W. Yang and R. G. Parr, *Phys. Rev. B*, 1988, **37**, 785.
39 A. Schaefer, C. Huber and R. Ahlrichs, *J. Chem. Phys*., 1994, **100**, 5829.
40 A. Schaefer, H. Horn and R. Ahlrichs, *J. Chem. Phys*., 1992, **97**, 2571.
41 Z. H. Ni, H. Z. Kou, Y. H. Zhao, L. Zheng, R. J. Wang, A. L. Cui and O. Sato, *Inorg. Chem*., 2005, **44**, 2050.
42 (*a*) O. Kahn and B. Briat, *J. Chem. Soc., Faraday Trans*., 1976, **72**, 268; (*b*) J. J. Girerd, Y. Journaux and O. Kahn, *Chem. Phys. Lett*., 1981, **82**, 534.
43 H. Chevreau, I. de P. R. Moreira, B. Silvi and F. Illas, *J. Phys. Chem. A*, 2001, **105**, 3570.
44 J. Cabrero, N. Ben Amor, C. de Graff, F. Illas and R. Caballol, *J. Phys. Chem. A*, 2000, **104**, 9983.
45 O. Kahn, *Molecular Magnetism*, VCH, New York, 1993, pp. 145–183.